技 術 報 告

無水ヒドラジンを用いた TiN ALD (原子層堆積法) プロセス

Atomic Layer Deposition Process of Titanium Nitride Using an Ultra-Dry Hydrazine Gas

村田逸人*　清水秀治*　安達啓輔**
MURATA Hayato　SHIMIZU Hideharu　ANDACHI Keisuke
ダニエル アルヴァレズ ジュニア***　ジェフェリー スピージェルマン***　鈴木克昌*
Daniel ALVAREZ Jr.　Jeffrey SPIEGELMAN　SUZUKI Katsumasa

半導体デバイスを構成する金属窒化膜の製造において，プロセス特性および膜質の改善が求められており，NH_3 代替として無水ヒドラジン (N_2H_4) の利用が期待されている。本稿では，安全・安定に無水ヒドラジンガスを供給できる RASIRC 製 BRUTE Hydrazine Vaporizer ™(BHV)を用いた TiN ALD 評価に関して報告し，NH_3 に対する N_2H_4 の優位性について議論する。具体的には，TiN 膜が形成され始めるインキュベーションタイム，TiN 膜の表面粗さ，および成膜速度 (GPC) が改善されることを確認した。加えて，NH_3 を用いて 400°C で形成した TiN 膜と比較し，N_2H_4 を用いて 300°C で形成した TiN 膜の抵抗率は低くなり，プロセス低温化と導電性改善を同時達成できることを示した。

In the process of metal nitride films formulation of the semiconductor devices, anhydrous hydrazine (N_2H_4) which is expected to improve the nitride films property is gaining an attention as an alternative to NH_3. In this paper, we report the improvement of TiN ALD films using N_2H_4 over NH_3. High purity N_2H_4 is delivered from BRUTE Hydrazine Vaporizer ™ (BHV) developed by RASIRC Corporation, which enables stable delivery of anhydrous hydrazine gas safely. From the experimental results, it was specifically confirmed that the incubation time when the TiN film starts to be formed, the surface roughness of the TiN film, and the growth per cycle (GPC) are improved. In addition, the resistivity of the TiN film formed at 300 °C using N_2H_4 was lower than that of the TiN film formed at 400 °C using NH_3, indicating that both process temperature reduction and conductivity improvement can be achieved at the same time.

1. INTRODUCTION

Atomic layer deposition (ALD), which enables superior film thickness control and step coverage, has been widely used in recent years with the miniaturization and structural complexity of semiconductor devices [1-4]. Metal nitride thin films to constitute a semiconductor device are conventionally formed by the ALD method using NH_3 gas as a nitriding agent. For example, TiN film is one of the important metal thin films to constitute a semiconductor device and functions as a barrier film around the wiring layer in the interconnects and capacitor electrodes for memory cells [5,6].

Although TiN ALD has already been employed in mass production of the semicoductor devices, lowering the temperature of the TiN ALD process and improving TiN film properties, such as lower resistivity, smaller surface roughness and good adhesiveness are required due to the advancement in the miniaturization of 3D transistor structures and the high degree of integration of 3D-NAND quired [7].

It is generally difficult to lower the temperature of TiN ALD process which uses $TiCl_4$ as a Ti precursor and NH_3 as a nitriding agent because $TiCl_4$-drived chlorine (Cl) remains in the TiN film. At temperatures below 400 °C, electrical

* 開発本部 つくば研究所 電子機材技術部 技術課
** 開発本部 事業開発統括部 事業開発部 イノベーション課
*** RASIRC Inc.

resistivity of TiN becomes higher since Cl impurity increases [8-11]. Therefore, new Ti precursors and new nitriding agent have been widely developed to improve the TiN film quality and to lower the process temperature simultaneously [12-17].

Amongst various nitriding agents, hydrazine is gaining an attention because its higher reactivity than NH_3 is expected to lower the film formation temperature and improve the film quality and throughput [18-20]. However, few reports have been made on TiN ALD process technology using N_2H_4, and the superiority over the conventional nitriding agent, NH_3, has not been fully discussed [21-22]. This is because high-purity anhydrous hydrazine required in the semiconductor manufacturing process is difficult to distribute and store.

To address the issues above, we performed the evaluation of TiN ALD using BRUTE Hydrazine Vaporizer ™ (RASIRC, Inc.) which enables stable and safe distribution of high-purity anhydrous hydrazine. In this paper, we report the ALD characteristics of TiN using NH_3 and N_2H_4, respectively, and discuss the superior characteristics of N_2H_4 over NH_3.

2. BRUTE Hydrazine Vaporizer™

Anhydrous hydrazine is generally difficult to handle from a safety perspective due to its strong toxicity and flammability. Because of its dangerous property, there are strict international regulations and domestic regulation in each country regarding the storage and transportation of hydrazine. For these issues, RASIRC Inc. commercialized BRUTE Hydrazine Vaporizer ™ which enables stable delivery of anhydrous hydrazine gas safely [23-24]. The features are as follows.

1) High-purity anhydrous hydrazine is filled.
2) Anhydrous hydrazine is stabilized by mixing with a proprietary solvent (shown in Fig.1)
3) Solvent remains in liquid phase due to its very low vapor pressure and does not evaporate into gas phase of hydrazine.
4) BRUTE system can deliver very high purity gas phase hydrazine with less than 1ppm of H_2O as a contaminant.

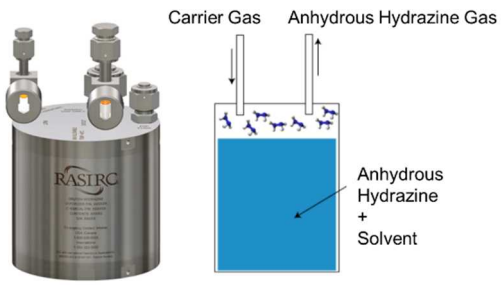

Fig. 1 BRUTE Hydrazine Vaporizer ™

3. EXPERIMENTAL

Fig. 2 and Table 1 show a schematic diagram and experimental conditions of our ALD system, respectively. $TiCl_4$ (99.999wt%, Japan Advanced Chemical) as a titanium precursor and NH_3 (99.999%, JAPAN FINE PRODUCTS) or N_2H_4 (BRUTE Hydrazine Vaporizer ™, RASIRC) as a nitriding agent were used. These process gases and purge gas were introduced alternately into a hot-wall tubular reactor according to the flow sequence shown in Fig. 2. A silicon wafer or a 100-nm thermal silicon oxide film deposited on a silicon wafer was used as a substrate.

Growth per cycle (GPC), refractive index (R.I.), surface roughness, impurities in TiN films and electrical conductivity were evaluated as TiN-ALD characteristics. GPC was calculated from the film thickness and the number of ALD cycles. A spectroscopic ellipsometer was used to measure the film thickness and R.I.. AFM (atomic force microscopy) and SIMS (secondary ion mass spectrometry) were used to measure the surface roughness and the amount of impurities of TiN films, respectively. The film conductivity was evaluated based on the electrical resistivity measured using four-point probe method.

In addition, we investigated pyrolysis characteristics of N_2H_4 gas. The chemical species in the exhaust gas were measured by Q-MS (quadruple mass spectrometry) installed at the downstream of the hot-wall tubular reactor.

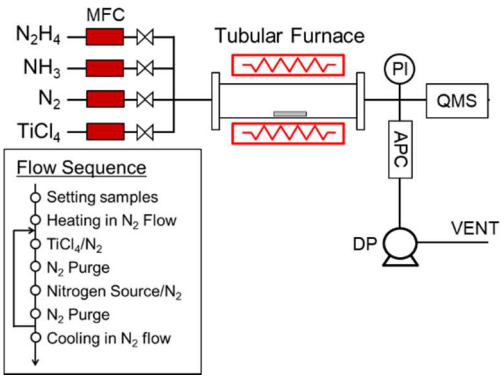

Fig. 2 Schematic diagram of ALD system

Table 1　ALD process conditions

Parameter	Range
Total Pressure	133 Pa
Temperature	250 - 400ºC
Number of ALD Cycles	120 - 2000
Precursor	$TiCl_4$
Partial Pressure	0.5 Pa
Feeding Time	2 - 15 s
Nitrogen Source	1) N_2H_4
	2) NH_3
Partial Pressure	5.3 Pa
Feeding Time	2 - 10 s

4.　RESULTS AND DISCUSSION

4.1　TiN Thickness Controllability

Fig. 3 shows that GPC of TiN film is almost constant under the condition of $TiCl_4$ feeding time over 2s. This means that $TiCl_4$ adsorption was saturated by feeding $TiCl_4$ for 2s or more and that TiN thin film was formed in ALD mode under temperature range of 250-400 °C. In the following experiments, $TiCl_4$ feeding time was set to 2 s based on this result. Fig. 4 shows correlation between TiN thickness on Si substrate and the number of ALD cycles. The regression lines show good linearity with determination coefficient $R^2 > 0.999$ under each condition. This means that TiN thickness could be preciselly controlled by the number of ALD cycles.

Fig. 5 shows correlation between TiN thickness on thermal silicon oxide film and the number of ALD cycles. X-intercepts in Fig.5 are known as the incbation cyle, during which initial nucleation was reported to take place on substrate surface before a film begins to grow [25]. In our TiN ALD evaluation, the incubation cycle clearly depends on the nitriding agents. Although the film thickness measurement might contain errors for each regression line, $TiCl_4/N_2H_4$ ALD has fewer incubation cycles than $TiCl_4/NH_3$ ALD at intersection point of the regression lines with X-axis. Hence, the use of N_2H_4, which has a higher nitriding ability than NH_3, facilitated nucleation and shortened the incubation cycle.

Fig. 6 shows surface roughness of 100nm thermal silicon oxide film and TiN films formed on that. The tendency of Root-Mean-Square-roughness (RMS) is similar to that of Maximum-Roughness-Depth (Rmax). The TiN film formed under conventional condition, which is NH_3 and 400 °C, has the larger roughness than the other TiN films using N_2H_4. Surface roughness reflects a growth mode; for instance, the island growth mode through local nucleation as shown in Fig. 7 leads to higher roughness[25-26]. Therefore, our experimental result indicates that N_2H_4 is likely to inhibt the island growth mode, lowering the surface roughness.

As mentioned above, it is considered that $TiCl_4$/ N_2H_4 ALD is more suitable to form an ultrathin film than $TiCl_4/NH_3$ ALD since the incubation cycle is reduced and the surface roughness is improved.

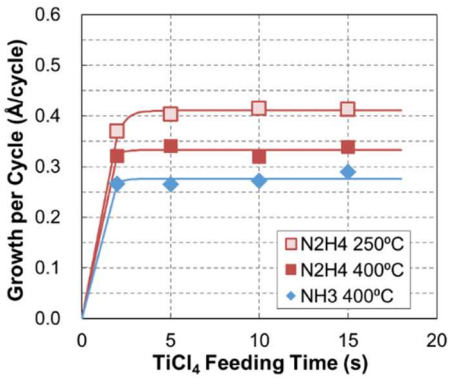

Fig. 3　TiCl4 feeding time dependence of GPC

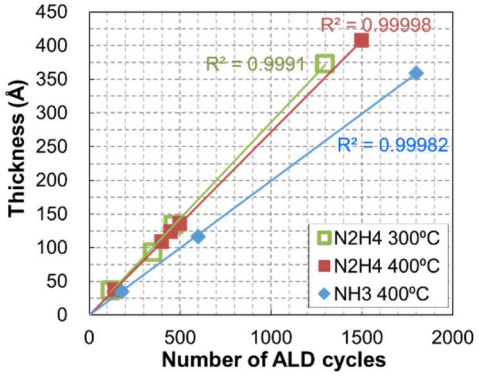

Fig. 4　ALD cycles dependence of TiN thickness

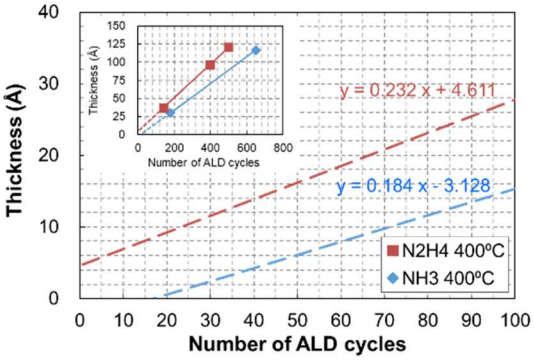

Fig. 5　ALD cycles dependence of TiN thickness

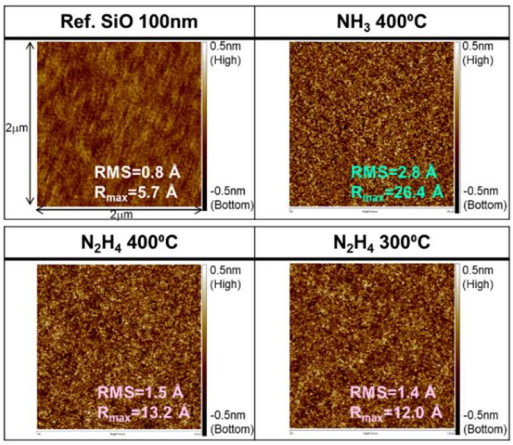

Fig. 6　Surface roughness

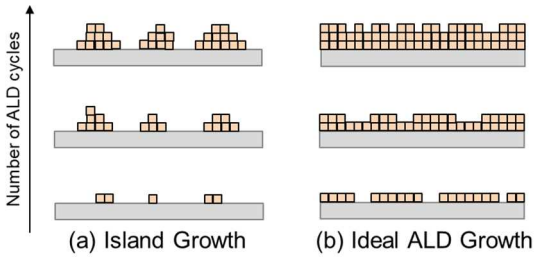

Fig. 7　Schematic of Island growth [25)]

4.2　Deposition Rate and N_2H_4 Pyrolysis Characteristics

Fig. 8 shows deposition-temperature dependence of GPC. GPCs in $TiCl_4/N_2H_4$ ALD were found to be 0.42-0.32 Å/cycle while those in $TiCl_4/NH_3$ ALD were 0.10-0.27 Å/cycle at 250-400 °C. Interestingly, the GPC in $TiCl_4/N_2H_4$ ALD is lower at higher temperature. To understand the chemical mechanism of the decrease in the GPCs with temperature, we investigated gas-phase reaction of N_2H_4 in the ALD process and an effect of the gas-phase reaction on GPC.

Temperature dependence of N_2H_4 decomposition ratio is shown in Fig. 9. The N_2H_4 decomposition ratio was lower at higher temperature, correlating to the temperature dependence of GPC of $TiCl_4/N_2H_4$ ALD. It was found that the effective N_2H_4 ratio contributed to the film formation reaction is only 45% in the case of 400 °C and 90% in the case of 250 °C. In addition, as shown in Fig. 10, it was confirmed by experiments that the N_2H_4 decomposition could be suppressed as the flow velocity increases. The tendency was the same at both 300 °C and 500 °C.

From these results, it is considered further improvement of GPC could be available by preventing the decomposition of N_2H_4 before reaching to the substrate.

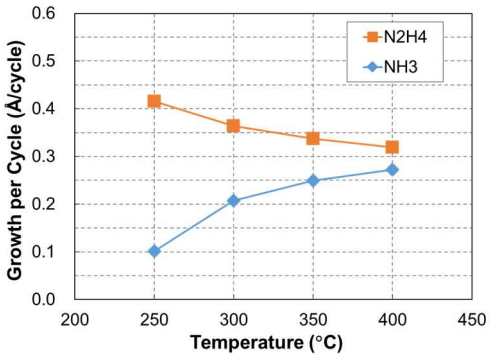

Fig. 8　ALD temperature dependence of GPC

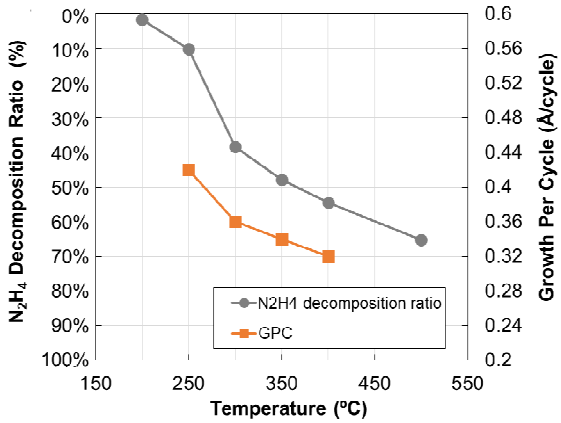

Fig. 9　ALD temperature dependence of N_2H_4 decomposition ratio

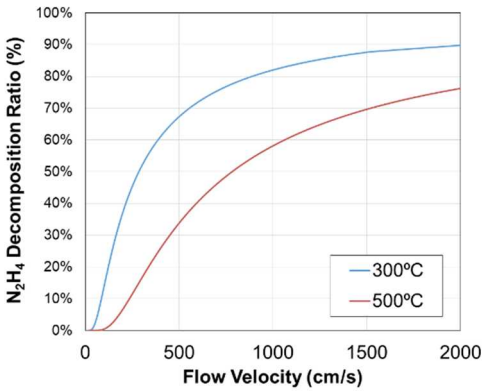

Fig. 10　Flow velocity dependence of N_2H_4 decomposition ratio

4.3　TiN Film Quality

Table 2 shows impurities in the TiN film. The amount of chlorine (Cl) in the TiN film is smaller at the condition of higher deposition temperature and using N_2H_4. To verify this

mechanism, the reactivity of the $TiCl_4$ adsorption structure on the substrate surface with nitriding agent, which is NH_3 or N_2H_4, was calculated by a theoretical chemical calculation method. Gaussian16 was used as the calculation software with density functional theory B3LYP and cc-pVDZ basis set. The results shown the following support that N_2H_4 is more likely to react with Ti-Cl bonds on the substrate surface.

$$=\text{Ti-Cl} + NH_3 \rightarrow =\text{Ti-}NH_2 + HCl \quad \Delta H = 33 \text{ kJ/mol}$$

$$=\text{Ti-Cl} + N_2H_4 \rightarrow =\text{Ti-}NHNH_2 + HCl \quad \Delta H = -28 \text{ kJ/mol}$$

Fig. 11 shows the temperature dependence of the refractive index (R.I.) of TiN films. The TiN films formed using $TiCl_4/N_2H_4$ at 250-400 °C likely had as good quality as typical sputtered TiN whose R.I. is about 1.66. In contrast, R.I. of $TiCl_4/NH_3$ film indicates that poorer-quality TiN film was formed at lower deposition temperature. Specifically, R.I. was larger than 2.00 in the case of $TiCl_4/NH_3$ ALD at 250-300 °C. These results suggest a mechanism that $TiCl_4/NH_3$ ALD has more Ti-Cl bonds as the film formation temperature is lower and forms titanium oxide [27] whose R.I. is 2.4-2.5 by reacting with air at outside of chamber. In other words, when N_2H_4 is used, it is considered that the good-quality TiN film was formed even at 300 °C or less due to its strong nitriding ability.

Fig. 12 shows the electric resistivity of the TiN film. The electric resistivity of the TiN film is lower at the condition of higher deposition temperature and using N_2H_4. Especially, it is worth mentioning that the electric resistivity of 442 ohm-cm in the case of using N_2H_4 at 300 °C is lower than that of 568 ohm-cm in the case of using NH_3 at 400 °C.

As mentioned above, $TiCl_4/N_2H_4$ ALD is more suitable to form a high-quality TiN film than $TiCl_4/NH_3$ ALD since the lower impurities and the lower resistance can be achieved at lower deposition temperature.

Table 2　Impurities in TiN film

	Cl(%)	O(%)	H(%)
NH_3 400 °C	0.88	6.07	0.04
NH_3 300 °C	7.46	9.63	0.67
N_2H_4 400 °C	0.69	4.41	0.07
N_2H_4 300 °C	2.09	4.37	1.08

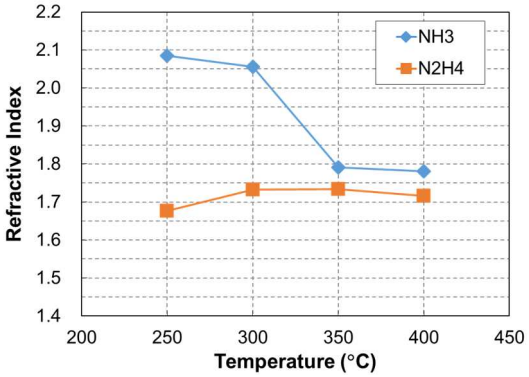

Fig. 11　ALD temperature dependence of R.I.

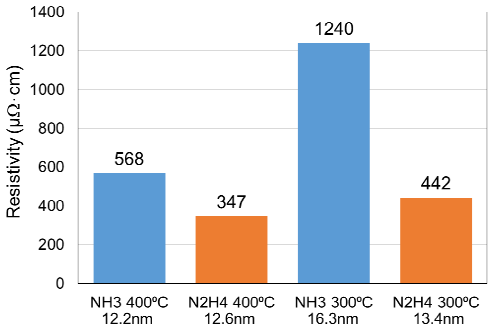

Fig. 12　Electric resistivity of TiN films

5.　CONCLUSION

The effectiveness of N_2H_4 on the TiN ALD process was verified using RASIRC's BRUTE Hydrazine Vaporizer ™ (BHV). The characteristics of TiN-ALD using $TiCl_4/N_2H_4$ were compared with that using $TiCl_4/NH_3$ at deposition temperature range of 250 to 400 °C.

It was shown that the incubation cycle was reduced and the surface roughness was improved by using N_2H_4 as an alternative to NH_3. These results mean that $TiCl_4/N_2H_4$ ALD is superior to form an ultrathin film than $TiCl_4/NH_3$ ALD. GPCs in $TiCl_4/N_2H_4$ ALD were higher than those in $TiCl_4/NH_3$ ALD. In addition, it was confirmed that GPC of $TiCl_4/N_2H_4$ ALD was elevated under the condition where thermal decomposition of N_2H_4 was prevented. Lower impurities and lower resistance were achieved at lower deposition temperature by using N_2H_4 when compared to NH_3.

Thus, anhydrous N_2H_4 is expected to improve both throughput of ALD and quality of nitride ALD films simultaneously.

Reference

1）Steven M. George, Chem. Rev., 110, 111–131, 2010.
2) V. Miikkulainen, M. Leskela, M. Ritala, R. L. Puurunen, Appl. Phys., 113, 021301, 2013.
3) R. W. Johnson, A. Hultqvist, S. F. Bent, Materials Today, Volume 17, 236, 2014.
4) H. B. Profijt, S. E. Potts, M. C. M. van de Sanden, W. M. M. Kessels, J. Vac. Sci. Technol. A, 29(5), 050801, 2011.
5) M. Harada, Y. Ogawa, S. Toyoda, H. Ushikawa, ULVAC TECHNICAL JOURNAL, No.70E 2009.
6) K. E. Elers, J. Winkler, K. Weeks, S. Marcus, J. Electrochem., 152(8), G589, 2005.
7) D. Alvarez Jr., et al., ECS Transactions, 77, 219, 2017.
8) S. Xie, J. Cai, Q. Wang, L. Wang, Z. Liu, , Tsinghua Sci Technol, 19(2), 144, 2014.
9) C. H. Ahn, S. G. Cho, H. J. Lee, K. H. Park, S. H. Jeong, Met. Mater. Int., Vol. 7, 621, 2001.
10) H. Tiznado, F. Zaera, J. Phys. Chem. B, 110, 13491, 2006.
11) D. Jeong, J. Hwang, H. Chae, J. Korean Phys. Soc., 54(3), 1087, 2009.
12) H. K. Kim, J. Y. Kim, J. Y. Park, Y. Kim, Y. D. Kim, H. Jeon, J. Korean Phys. Soc., 41(5), 739, 2002.
13) J. Y. Kim, G. H. Choi, Y. D. Kim, Y. Kim, and H. Jeon, Jpn. J. Appl. Phys., 42, 4245, 2003.
14) D. J. Kim, Y. B. Jung, M. B. Lee, Y. H. Lee, J. H. Lee, J. H. Lee, Thin Solid Films 372, 276, 2000.
15) M. Juppo, M. Ritala, M. Leskela, J. Electrochem., 147(9), 3377, 2000.
16) T. Kato, Z. Ni, M. Matsukuma, H. Nakamura, Y. Ideno , Y. Serizawa, The AVS 19th International Conference on Atomic Layer Deposition, South Korea, TF+AP-TuM11, 2019.
17) M. Juppo, P. Alen, M. Ritala, T. Sajavaara, J. Keinonen, and M. Leskela, Electrochem. Solid-State Lett. 5, C4, 2002.
18) B. B. Burton, A. R. Lavoie, S. M. George, J. Electrochem., 155(7), D508, 2008.
19) W. Yeh, R. Ishihara, S. Morishita, M. Matsumura, J. Appl. Phys, 35, 1509, 1996.
20) S. Morishita, S. Sugahara, M. Matsumura, Applied Surface Science 112, 198–204, 1997.
21) S. Wolfa, M. Breedena, I. Kwaka, J. H. Parka, M. Kavrika, M. Naikc, D. Alvarezd, J. Spiegelmand, A. C. Kummela, Appl. Surf. Sci., 462, 1029, 2018.
22) A. Hinckley, A. Muscat, Solid State Phenomena, 282, 232, 2018.
23) J. Spiegelman, D. Alvarez, K. Andachi; A. Lucero, A. Kondusamy, S. M. Hwang, X. Meng, H. Kim, J. Kim, The AVS 18th International Conference on Atomic Layer Deposition, AM-TuP-2, 2018.
24) D. Alvarez, et al., ECS Transactions, 72(4), 243, 2016.
25) R. L. Puurunena, J. Appl. Phys. 97, 121301, 2005.
26) R. L. Puurunena, W. Vandervorst, J. Appl. Phys. 96, 7686, 2004.
27) D. Alvarez Jr., J. Spiegelman, K. Andachi, G. Tsuchibuti, K. Suzuki, SPIE Advanced Lithography Conference, 11326-27, 2020.